



ELSEVIER

Contents lists available at ScienceDirect

Journal of Fluids and Structures

journal homepage: www.elsevier.com/locate/jfs

Vortex shedding and three-dimensional behaviour of flow past a cylinder confined in a channel

Martin D. Griffith^{a,*}, Justin Leontini^a, Mark C. Thompson^a, Kerry Hourigan^{a,b}

^a Department of Mechanical and Aerospace Engineering, Monash University, Clayton 3800, VIC, Australia

^b Division of Biological Engineering, Monash University, Clayton 3800, VIC, Australia

ARTICLE INFO

Article history:

Received 15 October 2010

Received in revised form

21 February 2011

Accepted 21 February 2011

Available online 10 March 2011

Keywords:

Cylinder wake

Floquet linear stability

Channel flow

ABSTRACT

A numerical investigation of the flow past a circular cylinder centred in a two-dimensional channel of varying width is presented. For low Reynolds numbers, the flow is steady. For higher Reynolds numbers, vortices begin to shed periodically from the cylinder. In general, the Strouhal frequency of the shedding vortices increases with blockage ratio. In addition, a two-dimensional instability of the periodic vortex shedding is found, both empirically and by means of a Floquet stability analysis. The instability leads to a beating behaviour in the lift and drag coefficients of the cylinder, which occurs at a Reynolds number higher than the critical Reynolds number for the three-dimensional mode A-type instability, but lower than a Reynolds number for any mode B-type instability.

© 2011 Elsevier Ltd. All rights reserved.

1. Introduction

The flow around a circular cylinder confined in a two-dimensional channel presents several similarities and differences when compared to the more well-known case of the unconfined cylinder. Sahin and Owens (2004) presented a parameter space study detailing the transition from steady two-dimensional flow to periodic vortex shedding across a range of blockage ratio, and found that the critical Reynolds number for such a transition increased with increasing blockage ratio. At increased blockage ratios, the flow alters significantly, with vortices beginning to be shed from both the cylinder and the walls. Furthermore, steady asymmetric solutions were found at higher blockage ratios. Another notable phenomenon of the flow is the inversion of the von Kármán vortex street. At a given distance downstream of the cylinder, depending on the blockage ratio and the Reynolds number, a vortex will cross to the side of the channel opposite to the side from which it shed. This phenomenon has been observed in both two- and three-dimensional studies (Rehimi et al., 2008). As for the transition from two-dimensional to three-dimensional flow, for a single blockage ratio of 0.20, Camarri and Gianetti (2010) used linear stability analysis to show that the inversion had little effect on the types of mode of transition and that the critical Reynolds numbers and wavelengths were quantitatively similar to those of the unconfined case. They chose a blockage ratio of 0.20 in order to isolate the effects of the wake inversion on the three-dimensional dynamics.

Extending on the work of Sahin and Owens (2004), this article explores the two-dimensional dynamics of the periodic vortex shedding flow across a wide range of blockages. Also investigated is the three-dimensional behaviour at higher blockage ratios, where in addition to the wake inversion, the effect of vortices shed from the walls may become important.

* Corresponding author.

E-mail address: martin.griffith@eng.monash.edu.au (M.D. Griffith).

Section 2 will detail the parameters and numerical methods, Section 3 the results of the study and Section 4 the discussion and conclusions.

2. Method

Fig. 1 presents a sketch of the geometry under consideration. The Reynolds number is defined as $Re = U_c D / \nu$, where U_c is the maximum velocity of the inlet Poiseuille velocity profile, D is the diameter of the circular cylinder and ν is the kinematic viscosity. The blockage ratio is defined as $b = D/H$, where H is the width of the channel. The Reynolds number is varied between $0 < Re \leq 300$, and the blockage ratio from $0.1 \leq b \leq 0.9$.

A spectral-element solver is used to obtain two-dimensional solutions to the Navier–Stokes equations. The numerical method used is the same as used in our previous studies of constricted channel and pipe flow (Griffith et al., 2007, 2009). No slip boundary conditions are applied on the cylinder and the walls, a Poiseuille profile is applied at the inlet and a first order pressure gradient condition is applied at the outlet.

Details of the linear Floquet stability analysis employed in this paper can be found in Griffith et al. (2007), which uses the same technique. The method solves the linearized perturbation equations using the same numerical solver as for the base flow. For a given Reynolds number and perturbation wavenumber, k , the leading instability mode and corresponding Floquet multiplier, μ , are determined using a power method. A multiplier greater than one indicates that the flow is unstable for that given wavenumber and Reynolds number.

Inlet and outlet lengths of $L_i = 12D$ and $L_o = 45D$ are used. At the extreme of the Reynolds number range, the independence of the solution to mesh resolution was tested by increasing the polynomial order of the spectral-element solver. For each mesh, at increased resolution, changes in the Strouhal frequency ($St = f_0 D / U_c$, where f_0 is the vortex shedding frequency) and in instability Floquet multipliers were less than one percent of the value for the mesh resolution used in the following results.

3. Results

Across the blockage ratio range, Sahin and Owens (2004) provide the critical Reynolds numbers for the transition from a steady flow to a periodic vortex-shedding flow. The work presented here details the dynamics of these periodic flows. To that end, Fig. 2 plots the Strouhal frequency across the Reynolds number and blockage range tested. The Strouhal frequency is determined by performing a frequency analysis on a time series of the lift coefficient of the cylinder. In general, the Strouhal frequency increases with Reynolds number and blockage ratio. Flows for blockage ratio, $b = 0.90$, at the extreme of the blockage ratio range, exhibit a different behaviour, with Strouhal frequencies less than those observed for $b = 0.80$.

Fig. 3 presents plots of vorticity for three base flows for $Re = 188$ and three blockage ratios, $b = 0.20, 0.33$ and 0.50 . For the smallest blockage shown, $b = 0.20$, the wake bears similarity to the wake behind an unconfined cylinder. Vorticity is pulled from the walls, but only a small amount when compared to the other two cases. For blockage ratios $b = 0.33$ and 0.50 , vortices forming on the walls of the channel can be seen being entrained into the vortex street. Also discernible in the three cases is the inversion of the vortex street; vortices forming on one side of the cylinder finish further downstream on the opposite channel.

In all periodic cases shown there is a dominant Strouhal frequency. However, at higher Reynolds number and blockage ratios, a second frequency appears in the oscillating lift coefficient. Fig. 4(a) plots a time series of the lift coefficient for Reynolds number $Re = 300$ and blockage $b = 0.50$. A low frequency beating can be seen. This phenomenon is indicative of two unequal but similar frequencies in the signal. This is borne out in Fig. 4(b), which shows the corresponding power spectrum. Alongside the Strouhal frequency of $St = 0.513$ a second peak can be seen at $f \approx 0.468$. The difference between these two frequencies corresponds to the period of the beating in Fig. 4(a). The same beating is apparent in the time series of the drag coefficient.

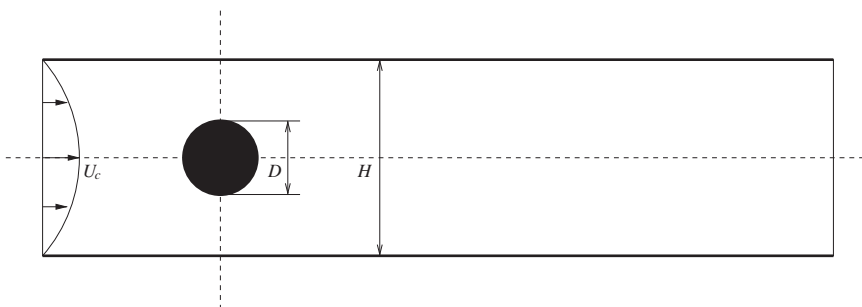


Fig. 1. Sketch of the geometry under consideration.

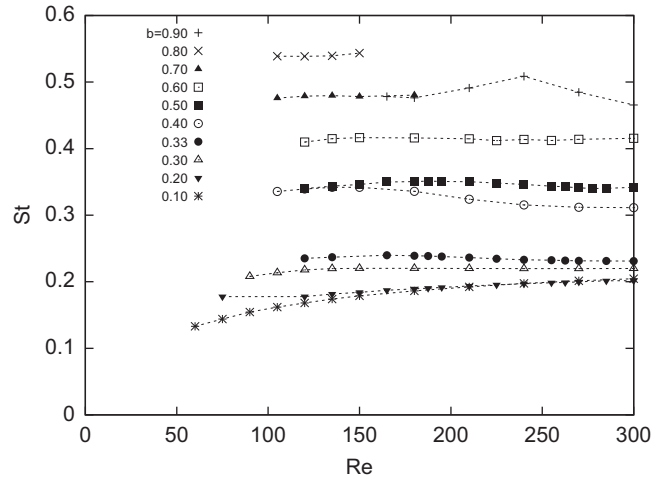


Fig. 2. Variation of Strouhal frequency for all periodic vortex shedding flow over the parameter range tested. Lines are added for clarity. Steady flows are not represented on the graph.

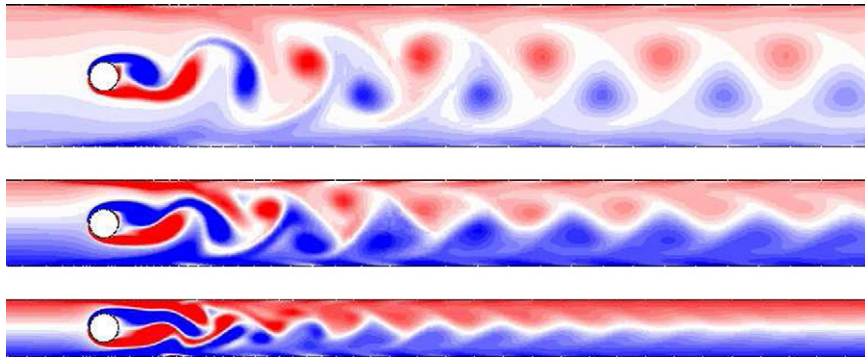


Fig. 3. Vorticity plots for three periodic flows for Reynolds number $Re=188$ and blockage ratios, top to bottom, $b=0.20, 0.33$ and 0.50 . Vorticity contour levels vary between $-4.5 \leq \omega_z \leq 4.5$.

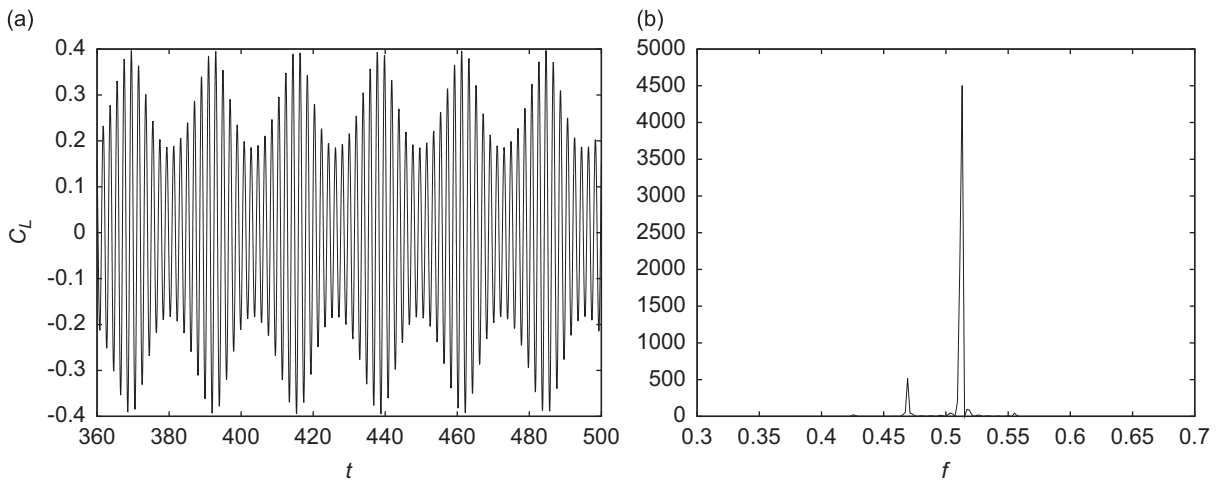


Fig. 4. (a) Time series of the lift coefficient for Reynolds number $Re=300$ and blockage ratio $b=0.50$ and (b) the corresponding power spectrum.

This phenomenon is explored further in Fig. 5. The figure shows vorticity plots separated by three periods corresponding to the dominant frequency of the flow ($3/St$). These images show the variation of the flow at the same phase; differences can be observed at $x \approx 3D$, the location of the detachment of the shedding vortices. Additionally, the strength of the vortices further downstream varies. In particular, in the second image the vortices appear confused and

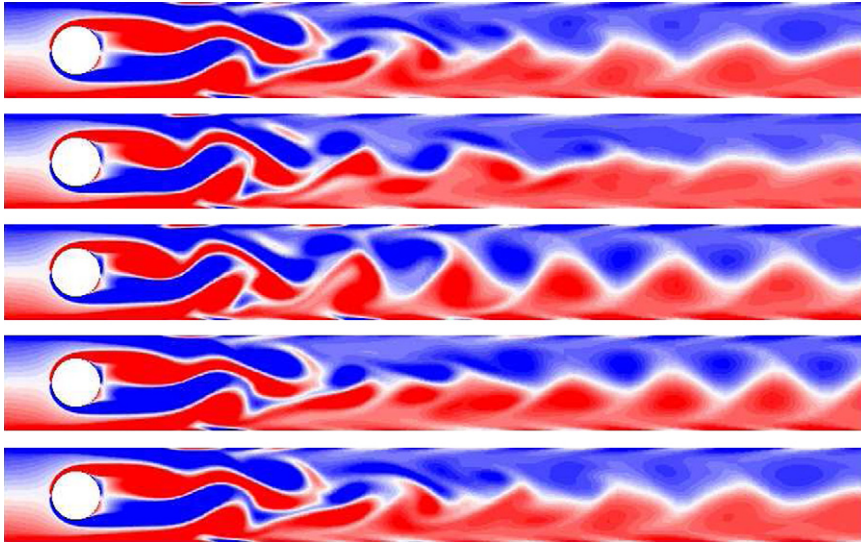


Fig. 5. Vorticity plots of the flow for Reynolds number $Re=300$ and blockage ratio $b=0.50$. Each image is separated by three periods of the dominant frequency $St=0.513$. Vorticity contour levels vary between $-4.5 \leq \omega_z \leq 4.5$.

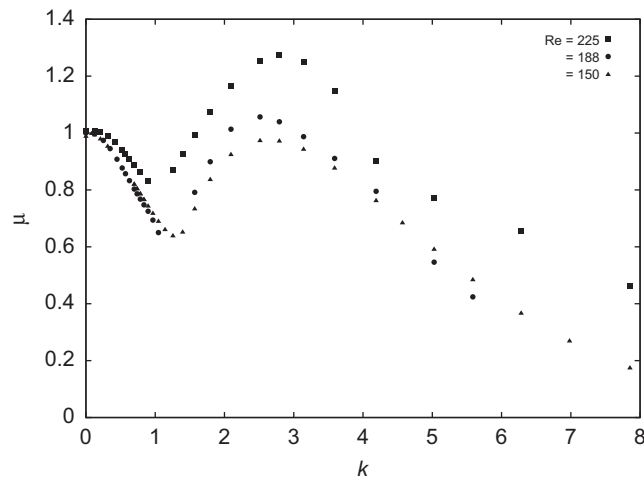


Fig. 6. Floquet multipliers across a range of Reynolds numbers for blockage ratio $b=0.50$.

counteractive, but in the third image are stronger and more ordered downstream. The first and last images are separated by 12 periods – approximately the period of the beating – and are nearly identical. The phenomenon was found to occur for Reynolds numbers greater than approximately 285.

The dominant frequency in the signal is related to the cylinder vortex shedding; this is the frequency plotted in Fig. 2 and there is a smooth variation of the frequency from Reynolds numbers where the beating is not present to Reynolds numbers where it is. The source of the second frequency may be due to the influence of the channel walls, and the vortices shed from it. For high enough Reynolds numbers, these vortices convect enough normal to the wall to begin to have an effect on the cylinder of the same order as the vortices that are shed directly from the cylinder.

For the same blockage ratio, $b=0.50$, Fig. 6 plots Floquet multipliers across three Reynolds numbers and a range of perturbation wavenumbers. The leading mode has a critical Reynolds number, $Re_c \approx 160$, with a wavenumber $k=2.65$. The mode bears similarity to the mode A instability typical of the flow around the unconfined cylinder, which is critical at a Reynolds number of 189 with a wavenumber of 1.59 (Barkley and Henderson, 1996). Characteristic of the mode A instability is its symmetry quality, expressed as $\hat{\omega}_x(x,y,k,t) = -\hat{\omega}_x(x,-y,k,t+T/2)$ (Blackburn et al., 2005). Beginning with the perturbation field at any time, advancing the flow half a base flow period in time, taking the negative of the vorticity and flipping the field around $y=0$ should yield an identical field. If the leading perturbation mode from Fig. 7 is a mode A instability and satisfies this condition, it should be apparent from plots of the velocity field taken $T/2$ apart. To that end,

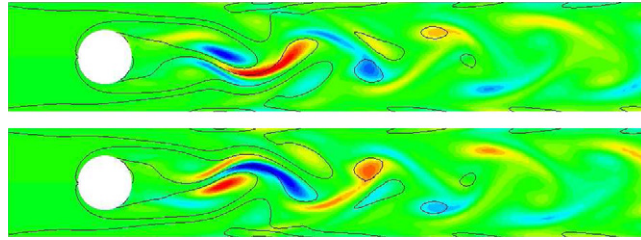


Fig. 7. Two plots of streamwise vorticity of the perturbation field for the flow for Reynolds number $Re=190$ and blockage ratio $b=0.50$, overlaid with vorticity representing the base flow. The bottom image is taken exactly one half-period after the top image.

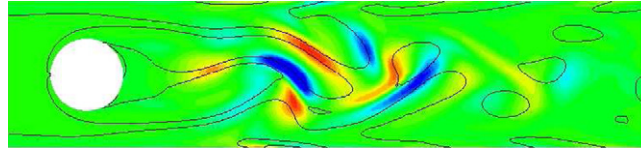


Fig. 8. Contours of spanwise vorticity of the two-dimensional perturbation field for the flow for Reynolds number $Re=188$ and blockage ratio $b=0.50$. Representative lines of the base flow vorticity are overlaid.

Fig. 7 contains two contour plots of the streamwise vorticity of the perturbation field for the flow for Reynolds number $Re=190$ and blockage $b=0.50$, with the second taken after an interval of half a period from the first. The case taken corresponds to the leading mode apparent from Fig. 6. In Fig. 7 one can discern the symmetry existing between the two images. The bottom image is the vertically reflected negative of the top, showing the mode satisfies the relation $\hat{\omega}_x(x, y, k, t) = -\hat{\omega}_x(x, -y, k, t + T/2)$, the same symmetry as exists for mode A in the unconfined case. In addition, the mode is at its strongest in the vortex cores. Along with the symmetry and similar critical Reynolds numbers and wavenumbers, this indicates that the instability mode is indeed of the same type as mode A in the unconfined case.

For the case of blockage $b=0.20$, Camarri and Gianetti (2010) reported results of a Floquet stability analysis, similar to that carried out here and summarized in Fig. 6. They reported that the behaviour of the Floquet multipliers for blockage $b=0.20$ was not markedly different to the behaviour in the unconfined case. This was despite the inversion of the downstream vortex stream. They concluded that the wake inversion has no significant effect on the stability because the cores of the instability modes are located in the near-wake region, where the wake vortices are still forming (Camarri and Gianetti, 2010). In the present results, for blockage $b=0.50$, the wake flow has altered more significantly than is the case for $b=0.20$. Not only is the wake inversion still present, but vortices are now being shed from the channel walls of the same order as those shed from the cylinder (see Fig. 3). The flow is altered enough from the unconfined case that the stability behaviour is noticeably affected – the mode B instability seen in the unconfined case and in the confined $b=0.20$ case is not evident in our stability analysis. Although it is possible that the mode B instability manifests at higher Reynolds numbers, there is certainly no evidence similar to what Camarri and Gianetti (2010) found for the case of blockage ratio $b=0.20$.

For the blockage ratio $b=0.50$, the stability analysis was carried out on flows up to the Reynolds number where the beating phenomenon shown earlier began. Given that the beating phenomenon occurs in our two-dimensional flow, evidence of the transition should appear in our Floquet stability analysis for wavenumbers $k=0$. Indeed, evidence of a two-dimensional $k=0$ instability can be seen in Fig. 6. Fig. 8 shows the leading two-dimensional $k=0$ perturbation mode for blockage $b=0.50$ and Reynolds number $Re=188$. In the figure, the perturbation is strongest in the region of the flow where we see the variation in the base flow in the in-phase images of Fig. 5. This indicates a strong link between the base flow behaviour for higher Reynolds numbers and the stability analysis. Note that for the case shown in Fig. 8, the flow is still periodic. Accordingly, the Floquet multiplier of this perturbation is less than one and the instability is decaying. The same analysis performed up to the critical Reynolds number $Re \approx 290$ returns multipliers fractionally less than one. This small decay rate results in the beating phenomenon appearing in the lift coefficient time series for $Re=285$. However, examination reveals the beating phenomena to be decaying, but only over a very long time scale.

For blockage ratios tested with $b \leq 0.40$, the beating phenomenon was not observed. For blockage ratio of $b=0.60$, the beating phenomenon is observable, yet can also be seen to be decaying slowly in the lift coefficient time series of flows for Reynolds numbers up to $Re \approx 240$.

4. Conclusions

The behaviour of the periodic two-dimensional flow around a cylinder confined in a channel, for various blockage ratios, has been investigated. The flow was characterized by the shedding behaviour; the Strouhal number increased with increasing blockage ratio. Also observed was a beating behaviour for the case of blockage ratio $b=0.50$ in the lift and drag coefficient time series; this is likely related to the effect of vortices shedding from the walls of the channel. Floquet

stability analysis was also performed for blockage ratio $b=0.50$. For a blockage ratio $b=0.20$, Camarri and Gianetti (2010) showed both mode A and mode B instabilities to exist at Reynolds numbers and wavenumbers similar to the unconfined case. For the case shown in most detail in this paper, $b=0.50$, the mode A instability can be found; however, the two-dimensional beating phenomenon begins at a Reynolds number lower than any Reynolds number where a mode B instability occurs. Further investigation will be performed, exploring in further depth the three-dimensional behaviour at other blockage ratios.

References

- Barkley, D., Henderson, R.D., 1996. Three-dimensional Floquet stability analysis of the wake of a circular cylinder. *Journal of Fluid Mechanics* 322, 215–241.
- Blackburn, H.M., Marques, F., Lopez, J.M., 2005. Symmetry breaking of two-dimensional time-periodic wakes. *Journal of Fluid Mechanics* 552, 395–411.
- Camarri, S., Gianetti, F., 2010. Effect of confinement on three-dimensional stability in the wake of a circular cylinder. *Journal of Fluid Mechanics* 642, 477–487.
- Griffith, M.D., Leweke, T., Thompson, M.C., Hourigan, K., 2009. Pulsatile flow in stenotic geometries: flow behaviour and stability. *Journal of Fluid Mechanics* 622, 291–320.
- Griffith, M.D., Thompson, M.C., Leweke, T., Hourigan, K., Anderson, W.P., 2007. Wake behaviour and instability of flow through a partially blocked channel. *Journal of Fluid Mechanics* 582, 319–340.
- Rehimi, F., Aloui, F., Nasrallah, S.B., Doubriez, L., Legrand, J., 2008. Experimental investigation of a confined flow downstream of a circular cylinder centred between two parallel walls. *Journal of Fluids and Structures* 24 (6), 855–882.
- Sahin, M., Owens, R.G., 2004. A numerical investigation of wall effects up to high blockage ratios on two-dimensional flow past a confined circular cylinder. *Physics of Fluids* 16, 1305–1320.